AD-A107 633 DAVID W TAYLOR NAVAL SHIP RESEARCH AND DEVELOPMENT CE--ETC F/G 20/11
AN EXPERIMENTAL EVALUATION OF TEARING INSTABILITY USING THE COM--ETC(U)
NOV 81 M G VASSILAROS, J A JOYCE
UNCLASSIFIED DTNSRDC-81/029 NL

1 OF 1
AD A
107633

END
DATE
FILMED
1 -82
DTIC

DTNSRDC-81/029

AD A107 633

AN EXPERIMENTAL EVALUATION OF TEARING INSTABILITY USING THE COMPACT SPECIMEN

DTIC FILE COPY

DAVID W. TAYLOR NAVAL SHIP RESEARCH AND DEVELOPMENT CENTER

Bethesda, Maryland 20084

AN EXPERIMENTAL EVALUATION OF TEARING INSTABILITY USING THE COMPACT SPECIMEN

by

Michael G. Vassilaros
James A. Joyce

APPROVED FOR PUBLIC RELEASE: DISTRIBUTION UNLIMITED

SHIP MATERIALS ENGINEERING DEPARTMENT
RESEARCH AND DEVELOPMENT REPORT

November 1981

DTNSRDC-81/029

MAJOR DTNSRDC ORGANIZATIONAL COMPONENTS

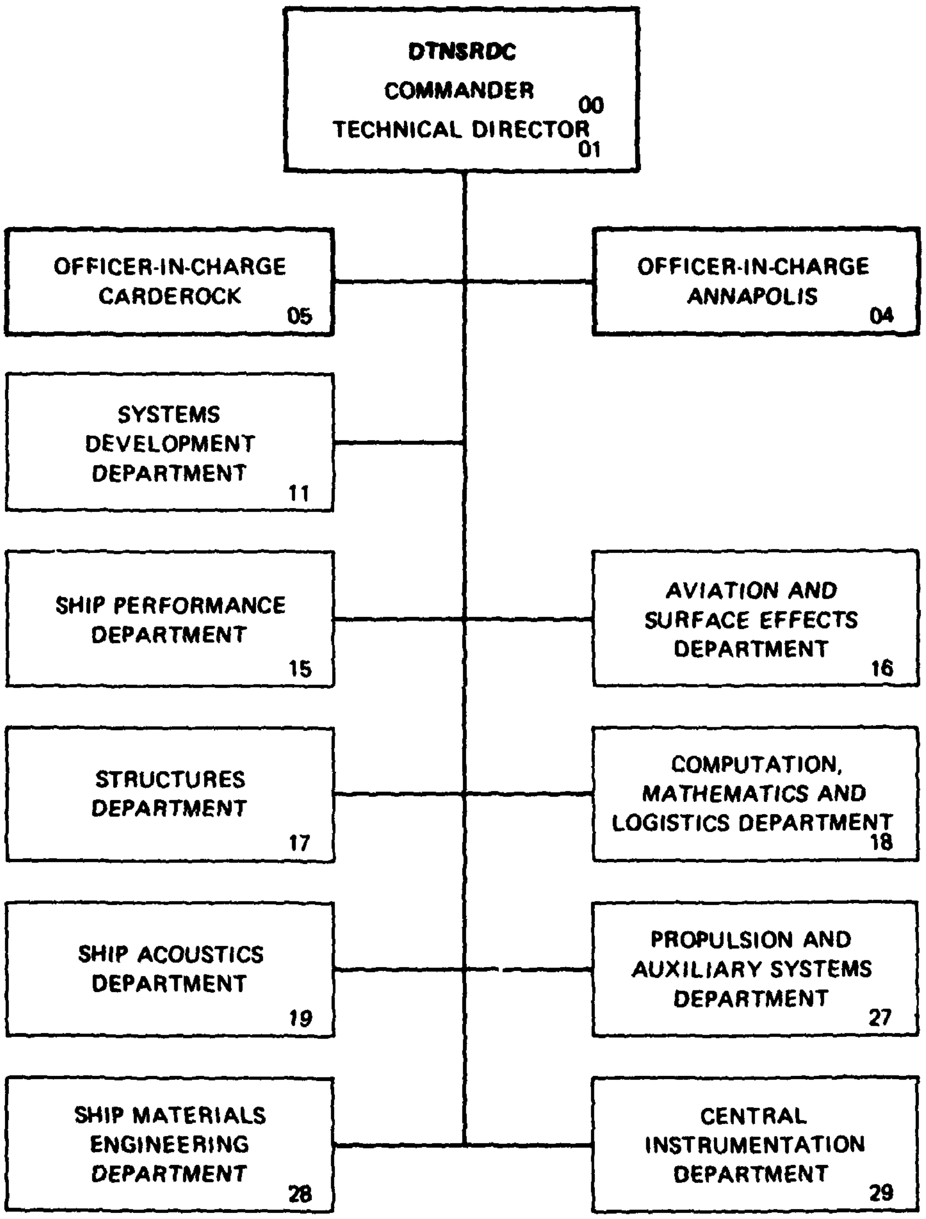

GPO 866 993

NDW-DTNSRDC 3960/43 (Rev. 2-80)

REPORT DOCUMENTATION PAGE		READ INSTRUCTIONS BEFORE COMPLETING FORM
1. REPORT NUMBER DTNSRDC-81/029	2. GOVT ACCESSION NO. AD-A107633	3. RECIPIENT'S CATALOG NUMBER
4. TITLE (and Subtitle) AN EXPERIMENTAL EVALUATION OF TEARING INSTABILITY USING THE COMPACT SPECIMEN		5. TYPE OF REPORT & PERIOD COVERED Final 6. PERFORMING ORG. REPORT NUMBER
7. AUTHOR(s) Michael G. Vassilaros James A. Joyce		8. CONTRACT OR GRANT NUMBER(s)
9. PERFORMING ORGANIZATION NAME AND ADDRESS David W. Taylor Naval Ship Research and Development Center Bethesda, Maryland 20084		10. PROGRAM ELEMENT, PROJECT, TASK AREA & WORK UNIT NUMBERS (See reverse side)
11. CONTROLLING OFFICE NAME AND ADDRESS		12. REPORT DATE November 1981 13. NUMBER OF PAGES 27
14. MONITORING AGENCY NAME & ADDRESS(if different from Controlling Office)		15. SECURITY CLASS. (of this report) UNCLASSIFIED 15a. DECLASSIFICATION/DOWNGRADING SCHEDULE

16. DISTRIBUTION STATEMENT (of this Report)

APPROVED FOR PUBLIC RELEASE; DISTRIBUTION UNLIMITED

17. DISTRIBUTION STATEMENT (of the abstract entered in Block 20, if different from Report)

18. SUPPLEMENTARY NOTES

19. KEY WORDS (Continue on reverse side if necessary and identify by block number)

Fracture Crack Instability	Ductile Fracture
Tearing Instability	Crack Propagation
Tearing Modulus	Stable Crack Growth
Elastic-Plastic Fracture	Compact Tension Specimen

20. ABSTRACT (Continue on reverse side if necessary and identify by block number)

The objective of this investigation was to produce experimental verification of the tearing instability theory proposed by Paris and coworkers. This theory states that ductile crack extension will occur in an unstable fashion whenever the applied tearing force is greater than the material tearing resistance. In this investigation, a series of compact specimens of aluminum, titanium, and steel alloys were tested in a variably compliant test

(Continued on reverse side)

(Block 10)

Program Element 62761N
Project 20457
Task Area SF 61-541-592
Work Unit 2803-161

(Block 20 Continued)

machine to generate a range of applied tearing forces. The material tearing resistance was measured from the J_I-R curves of the stable specimens and compared to the applied tearing force necessary to generate ductile tearing instability in each material. The Paris theory was found to accurately predict the onset of gross instability behavior. Some limited instability behavior was found, however, at values of tearing force less than the average material tearing resistance obtained from an unloading compliance J_I-R curve test. Limited instability behavior was characterized by repeated short steps of rapid but ductile crack extension, separated by regions of slow stable tearing.

TABLE OF CONTENTS

LIST OF FIGURES

Page

LIST OF TABLES

ABSTRACT

The objective of this investigation was to produce experimental verification of the tearing instability theory proposed by Paris and coworkers. This theory states that ductile crack extension will occur in an unstable fashion whenever the applied tearing force is greater than the material tearing resistance. In this investigation, a series of compact specimens of aluminum, titanium, and steel alloys were tested in a variably compliant test machine to generate a range of applied tearing forces. The material tearing resistance was measured from the J_I-R curves of the stable specimens and compared to the applied tearing force necessary to generate ductile tearing instability in each material. The Paris theory was found to accurately predict the onset of gross instability behavior. Some limited instability behavior was found, however, at values of tearing force less than the average material tearing resistance obtained from an unloading compliance J_I-R curve test. Limited instability behavior was characterized by repeated short steps of rapid but ductile crack extension, separated by regions of slow stable tearing.

ADMINISTRATIVE INFORMATION

This report was prepared as part of the Surface Ship and Craft Materials Block Program under the sponsorship of Dr. H.H. Vanderveldt, Naval Ship Systems Command (SEA 05R15). The effort was performed at the David W. Taylor Naval Ship Research and Development Center under Program Element 62761N, Task Area SF 61-541-592, Project 20457, and Work Unit 2803-161.

INTRODUCTION

During the past few years, it has become increasingly common to characterize a material's resistance to static crack extension in terms of the J resistance curve (J-R curve) as introduced by Begley and Landes.[1*] The usual application of this J-R curve has been to extrapolate back to the crack initiation parameter, J_{Ic}, which is then considered to be a material parameter. Crack extension is avoided in the structural element by limiting applied loads to values which keep the J integral (J) parameter at existing cracks below the material J_{Ic} value.

---

*A complete listing of references is given on page 21.

In many applications, overloads can be envisioned which could reach or exceed the loading required to initiate ductile crack extension. An added requirement for structural integrity then is that the crack growth be stable and not self-propagating and that it cease immediately when the overload is removed.

To address this problem, Paris and coworkers[2] have defined a tearing modulus quantity T as

$$T = \frac{E}{\sigma_o^2} \frac{dJ}{da} \qquad (1)$$

where E = elastic modulus

σ_o = material flow stress

da = change in crack length

A material tearing modulus, $T_{material}$, can then be defined by taking dJ/da as the slope of the material J_I-R curve beyond J_{Ic}.

The applied tearing force, $T_{applied}$, depends upon the material properties, E, σ_o, and the value of dJ/da applied to the crack tip by the combination of crack geometry, type of loading, and structural stiffness. Calculations of $T_{applied}$ have been accomplished by Paris and coworkers[2-4] for several simple geometries.

The tearing instability theory of Paris[2] states that a flawed member will tear stably when it is beyond J_{Ic}, and at its limit load, as long as $T_{applied} < T_{material}$. Tearing instability will occur whenever $T_{applied} \geq T_{material}$.

The objective of this investigation is to evaluate the validity of the Paris tearing instability theory by testing a series of compact specimens in a test apparatus of variable compliance. A range of materials including aluminum, titanium, and steel alloys were chosen to encompass a broad range of elastic moduli. Both side-grooved and non-side-grooved specimens were tested because earlier work[5,6] demonstrated that this geometry modification had a distinct effect on the material J_I-R curve, tending to give lower $T_{material}$ values when side grooves were present. Application of a range of $T_{applied}$ values would allow the determination of whether or not the $T_{material}$ value was geometrically dependent; if not, which $T_{material}$ more accurately predicted the instability conditions. Two crack lengths were studied to verify the accuracy of the expression for $T_{applied}$ over a range of this variable, elastic modulus, flow stress, and machine stiffness.

For each material, standard single specimen J_I-R curves were developed using a stiff test machine and the technique of Joyce and Gudas[7] to characterize $T_{material}$ for each material tested. Then, by increasing the test machine compliance, $T_{applied}$ was increased until it exceeded the $T_{material}$ value, at which point the previously stable specimens would be expected to fail in a rapid, unstable, but ductile fashion. Previous work of this type has been completed for one type of steel using bend specimens by Paris et al.[8] For all tests, the J integral size criteria[9] were met to keep the tests initially in the region of J-controlled growth.[10]

For the compact specimen geometry, $T_{applied}$ was calculated in a compliant test machine using the general analysis scheme outlined by Paris et al,[2] assuming elastic, fully plastic material behavior. The details of this analysis are described in this report.

MATERIALS AND EXPERIMENTAL METHOD

The experimental tearing instability analysis study was performed on a series of 36 1T compact specimens machined in the T-L orientation. These plate materials, which were chosen to encompass a wide range of elastic moduli, included Al 5456 H117 aluminum, Ti-3Al-2.5V titanium alloy, HY-130 steel, and as-quenched ASTM A533B steel. The mechanical properties of the materials are presented in Table 1. All specimens were tested at room temperature except the as-quenched A533B which was tested at 150°C. The tests were performed with a screw-driven Tinius Olsen tensile machine modified with a variable-stiffness titanium spring in the load train as shown in Figure 1. The spring was composed of two titanium beams in series loaded in three-point bending. The spring stiffness was a function of the span distance between the two rollers.

All the J_I fracture tests were conducted using a single specimen computer-interactive unloading compliance method using a mini-computer for data acquisition and analysis as developed by Joyce and Gudas.[7] The results of each unloading compliance test were plots of load versus load-line crack-opening displacement, load versus test machine-head displacement, and a J_I-R curve which included corrections for crack growth[11] and for specimen rotation.[12] The expression for J_I incorporating the crack growth correction is as follows:

TABLE 1 - MECHANICAL PROPERTIES OF MATERIALS USED IN TEARING INSTABILITY STUDY

Material	Modulus (psi (MPa))	Flow Stress (ksi (MPa))	J_{Ic} (in-lb/in^2 (kJ/m^2))	$T_{material}$ with 20 Percent Side Grooves a	b	Yield Stress (ksi (MPa))	Tensile Stress (ksi (MPa))	Elongation in 2 In. (percent)
Al 5456 H117	10.3×10^6 (71×10^3)	42.5 (293)	177 (31)	12	4	34 (234)	51 (351)	19
Ti-3Al-2.5V	15.4×10^6 (106×10^3)	80.5 (555)	450 (79)	22	11	73 (503)	88 (607)	22
ASTM A533B Steel, As-Quenched	29×10^6 (200×10^3)	65 (448)	1500 (262)	36*	26*	51 (352)	79 (545)	30
HY-130 Steel	29×10^6 (200×10^3)	145 (999)	870 (152)	14	9	138 (951)	152 (1048)	20

*Non-side-grooved specimens.

Notes: 1. Values of a were calculated from J_I-R curve data with crack extensions up to 1.5 mm, $a_o/w = 0.65$.

2. Values of b were calculated from J_I-R curve data with crack extensions up to 5 mm, $a_o/w = 0.65$.

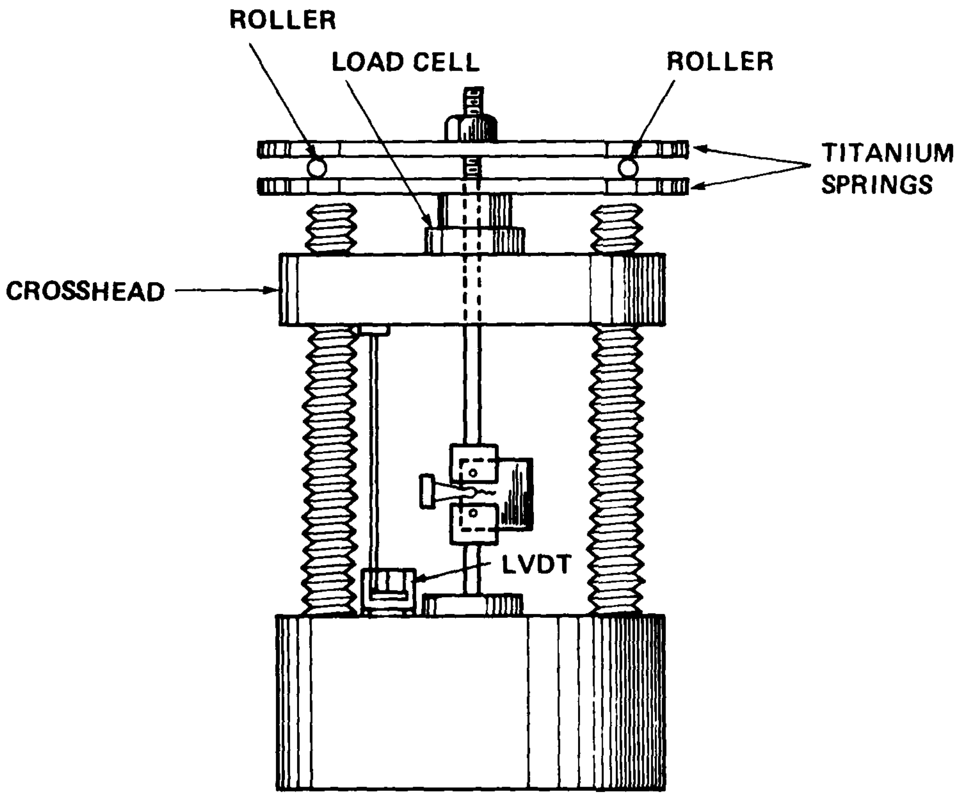

Figure 1 - Modified Screw-Driven Testing Machine

$$J_{(i+1)} = \left[J_i + \left(\frac{\eta}{b}\right)_i \frac{A_{i,i+1}}{B_N}\right] \left[1 - \left(\frac{1}{b}\right)_i (a_{i+1} - a_i)\right] \quad (\ )$$

where η = 2 + (0.522) b/W for compact specimens
W = specimen width

The computer program was modified to calculate machine compliance and $T_{applied}$ using the machined stiffness, applied J_I, and crack length from each unloading. Machine compliance was calculated by measuring the total system crosshead deflection versus applied load during the initial loading of a specimen, then subtracting the compliance contribution of the specimen. In addition to the digitally recorded data, an analog plot of load versus crosshead displacement was recorded during each test. This plot supplemented the load versus load-line crack-opening displacement (COD) curves and was used to identify instability events during the test. Table 2 is the test matrix for the tearing instability investigation which summarizes the materials, specimen geometries, and ranges of $T_{applied}$.

The $T_{material}$ values listed in Table 2 were calculated from conventional J_I-Integral tests in two ways. The first method was to use a least squares linear regression analysis as prescribed by Clarke et al.,[9] up to a crack extension of 1.5 mm, and the second method was to use a similar method but to include all test points up to a crack extension of 5 mm.

TEARING FORCE ANALYSIS

This section presents the derivation of an expression for the tearing force $T_{applied}$ for a compact specimen loaded in a compliant test machine.

For the specimen and test configuration shown in Figure 2, a fixed Δ_{TOT} is applied and held rigidly so that

$$\Delta_{TOT} = \Delta_{EL} + \Delta_{PL} + \Delta_M = \text{Constant} \quad (\ )$$

where Δ_{TOT}, Δ_{EL}, Δ_{PL}, and Δ_M are the total, elastic, plastic, and machine displacements, respectively.

TABLE 2 - RESULTS OF TEARING INSTABILITY STUDY ON 1T COMPACT SPECIMENS*

Material	a/W	Side Grooves (percent)	$T_{material}$	$T_{applied}$ at Maximum Load	Fracture Behavior
Al 5456 H117	0.65	0.0	19	3.5	Stable
				4.0	Semistable
				5.5	Semistable
				9.7	Semistable
				39.0	Unstable
Al 5456 H117	0.65	20.0	4	-1.4	Semistable
				1.5	Semistable
				4.7	Unstable
Al 5456 H117	0.80	0.0	17	-0.5	Stable
				4.7	Stable
				7.7	Semistable
				14.2	Semistable
				134.0	Unstable
Al 5456 H117	0.80	20.0	5	-7.2	Semistable
				3.4	Semistable
				10.0	Unstable
				21.0	Unstable
Ti-3Al-2.4V	0.65	0.0	20	-1.0	Stable
				6.0	Stable
				15.0	Stable
				29.0	Unstable
Ti-3Al-2.5V	0.65	20.0	11	-1.0	Stable
				5.0	Semistable
				13.0	Semistable
				17.0	Unstable
A533B (As-quenched; test at 300°F (150°C)	0.65	0.0	26	5	Stable
				5	Semistable
				23	Semistable
				34	Unstable
HY-130	0.65	0.0	22	3	Stable
				13	Semistable
				17	Semistable
				26	Unstable
				37	Unstable
HY-130	0.65	20.0	9	1.0	Semistable
				2.0	Semistable
				9.0	Semistable
				11.0	Unstable

*All tests conducted at room temperature except A533B tests.

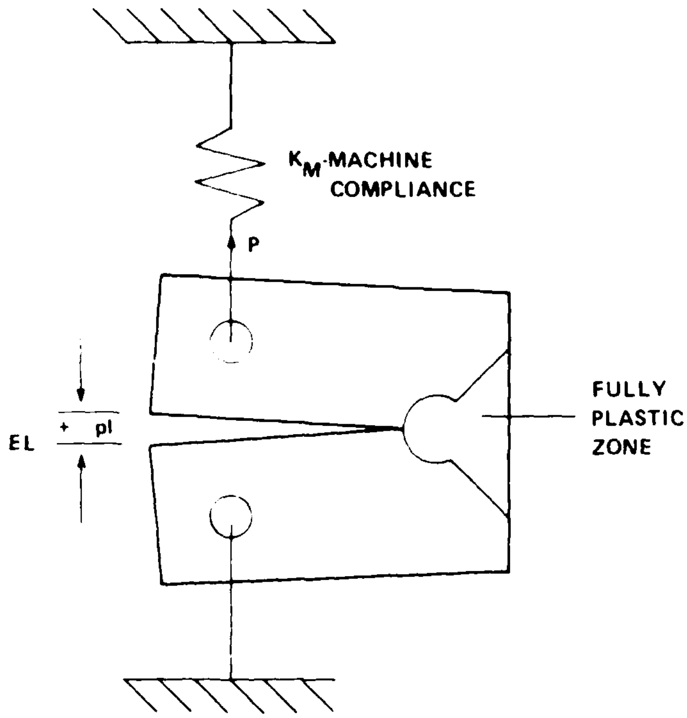

Figure 2 - Specimen Displacement Notation

During crack extension then, the sum of the differentials of Δ_{EL}, Δ_{PL}, and Δ_{M} must be zero, i.e.,

$$d\Delta_{EL} + d\Delta_{PL} + d\Delta_{M} = 0$$

For the compact specimen, the elastic displacement component can be evaluated from the relationship

$$\Delta_{EL} = \frac{P}{BE} \quad F\left(\frac{a}{W}\right)$$

where, from Saxena and Hudak,[13]

E = elastic modulus

B = specimen thickness

P = applied load

$$F\left(\frac{a}{W}\right) = \left(\frac{1+\frac{a}{W}}{1-\frac{a}{W}}\right)^2 \left[2.16299 + 12.219\,\frac{a}{W} - 20.065\left(\frac{a}{W}\right)^2\right. \tag{6}$$

$$\left. - 0.9925\left(\frac{a}{W}\right)^3 + 20.609\left(\frac{a}{W}\right)^4 - 9.9314\left(\frac{a}{W}\right)^5\right]$$

The plastic displacement component can be expressed as

$$\Delta_{PL} = \delta_t\, g\left(\frac{a}{W}\right) \tag{7}$$

where, from Merkle and Corten,[14]

$$g\left(\frac{a}{W}\right) = \left[\frac{2W}{W - a} + (\alpha - 1)\right] \frac{\delta_t}{1 + \alpha} \tag{8}$$

where δ_t = crack opening stretch

$$\alpha = \left\{[4a^2+4a(W-a)+2(W-a)^2]^{1/2}-(a+W)\right\} (W-a) \tag{9}$$

The testing machine is assumed here to behave like a linear elastic spring, so the testing machine displacement is given simply by

$$\Delta_M = \frac{P}{K_M} \tag{10}$$

where K_M, the machine stiffness, is a constant.

Assuming now that the load is at the specimen limit load, gives

$$P = P_L = \sigma_o BW\, h\left(\frac{a}{W}\right) \tag{11}$$

where, from Merkle and Corten,[14]

$$h\left(\frac{a}{W}\right) = \left(1 - \frac{a}{W}\right) \alpha \tag{12}$$

with α given by Equation (9). The final relationship needed is, from Paris[15] and Rice,[16] that the crack tip opening displacement is proportional to J as

$$\delta_t = \alpha^* \frac{J}{\sigma_o} \tag{13}$$

where α^* is a constant ≈ 1 for plane stress and ≈ 0.7 for plane strain.

Taking the differentials of Equations (5), (7), and (10), substituting into Equation (4), and rearranging gives the relationship

$$T_{applied} = \frac{E}{\sigma_o^2} \frac{\partial J}{\partial a} = - \frac{W}{a^* \, g\left(\frac{a}{W}\right)} \left\{ \frac{\partial}{\partial a} \left[h\left(\frac{a}{W}\right) \; f\left(\frac{a}{W}\right) \right] + \frac{EB}{K_M} \frac{\partial h\left(\frac{a}{W}\right)}{\partial a} + \frac{\alpha^* \, JE}{W \sigma_o^2} \frac{\partial g\left(\frac{a}{W}\right)}{\partial a} \right\} \tag{14}$$

where by differentiation of Equations (6), (8), and (12)

$$\frac{\partial f}{\partial a} = \frac{2}{W} \frac{1 + \frac{a}{W}}{1 - \frac{a}{W}} \frac{2}{\left(1 - \frac{a}{W}\right)^2} \left[2.16299 + 12.219 \frac{a}{W} - 20.065 \left(\frac{a}{W}\right)^2 - 0.9925 \left(\frac{a}{W}\right)^3 + 20.609 \left(\frac{a}{W}\right)^4 - 9.9314 \left(\frac{a}{W}\right)^5 \right] + \frac{1}{W} \left(\frac{1 + \frac{a}{W}}{1 - \frac{a}{W}} \right)^2 \left[12.219 - 40.13 \frac{a}{W} - 2.9775 \left(\frac{a}{W}\right)^2 + 82.436 \left(\frac{a}{W}\right)^3 - 49.657 \left(\frac{a}{W}\right)^4 \right] \tag{15}$$

$$\frac{\partial g}{\partial a} = \frac{\left\{1 + \frac{\partial[\alpha(W-a)]}{\partial a}\right\}[W-a + (W-a)\alpha]}{(W-a)^2\ (1+\alpha)^2}$$

$$- \frac{\left\{-1 + \frac{\partial[\alpha(W-a)]}{\partial a}\right\}[(W+a) + \alpha(W-a)]}{(W-a)^2\ (1+\alpha)^2} \tag{16}$$

$$\frac{\partial h}{\partial a} = \frac{1}{W}\ \frac{\partial[\alpha(W-a)]}{\partial a} \tag{17}$$

with, from Equation (9),

$$\frac{\partial[\alpha(W-a)]}{\partial a} = \frac{2a}{[4a^2 + 4a(W-a) + 2(W-a)^2]^{1/2}} - 1 \tag{18}$$

Substitution of Equations (15) through (18) into Equation (14) gives the final form of $T_{applied}$ used throughout this investigation, expressing the dependence of $T_{applied}$ on J_I, E, σ_o, a/W, and K_M for the compact specimen.

RESULTS AND DISCUSSION

DESCRIPTION OF SPECIMEN INSTABILITY BEHAVIOR

During the loading of the specimens described in the text, three general types of load versus displacement behavior were demonstrated as shown in Figure 3. The results shown in Figure 3a were from a J_I-R test performed in a rigid-test machine with the condition that $T_{material}$ was much greater than $T_{applied}$. The curve was constructed from digital data taken at 0.5 sec intervals. These data, regularly and closely spaced, reflect the stable response of the specimen to the constant crosshead rate used in all tests.

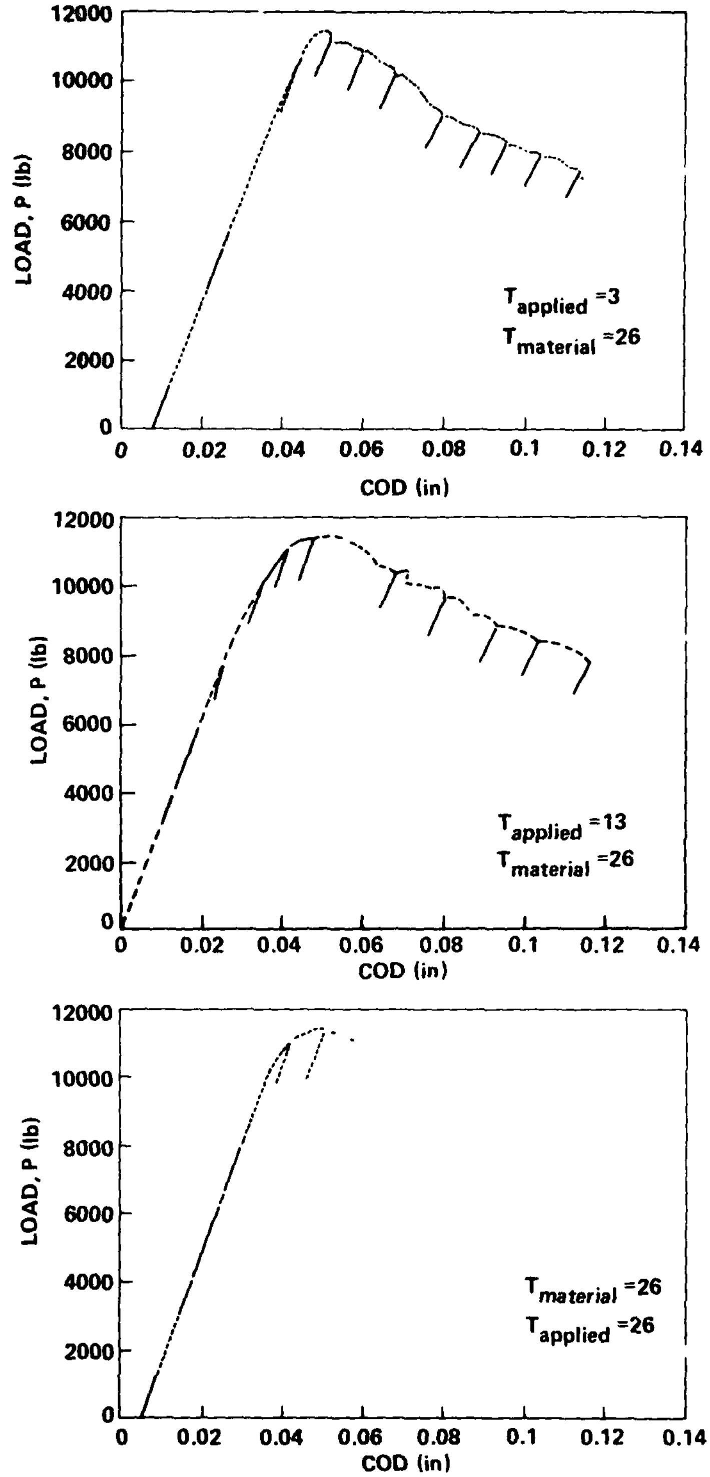

Figure 3 - Load Displacement Records for Three General Types of Tearing Behavior on HY-130 Steel

For the cases where $T_{applied}$ approached $T_{material}$ (but still less than $T_{material}$), the behavior shown in Figure 3b was observed. This behavior was characterized by repeated rapid steps of crack growth of relatively small magnitude, typically on the order of 0.1 mm to 0.5 mm, with larger steps being observed as $T_{applied}$ more closely approached $T_{material}$. The quick jumps of crack growth appeared as gaps in the load versus COD plot shown in Figure 3b. Each jump was accomplished in much less than the 0.5 sec data acquisition interval.

The specimens tested with $T_{applied} > T_{material}$ produced the type of load versus displacement shown in Figure 3c. At or near maximum load, instability occurred producing an increment of crack extension large enough to either separate the specimen completely or leave only a small remaining ligament. This sudden unstable crack extension is shown in Figure 3c as the blank region to the right of the load displacement plot.

Figures 3a and 3b show that the load displacement records for stable specimens and specimens with limited instability are similar in shape in spite of the presence of the small instabilities. Likewise, the J-R curves obtained from stable and limited instability specimens are similar in shape as shown in Figure 4 for the aluminum alloy. This insensitivity of the J_I-R curve to $T_{applied}$ was seen for all materials tested.

Both macroscopic observation and scanning electron microscopic analysis of the fracture surface of all materials studied here showed that the fracture surfaces were fully ductile and very similar whether they resulted from the stable tearing fracture or the rapid instability. No evidence of cleavage was observed in any of the test samples either near the beginning of the unstable tearing or during the growth of the rapidly propagating crack.

VERIFICATION OF INSTABILITY THEORY

The results of the complete series of tests are plotted in Figures 5 and 6 with each point representing a single specimen. Solid points denote specimens which demonstrated instability to such a degree that the test was stopped. The half-filled data points represent specimens which demonstrated limited instability.

The open data points represent specimens that behaved in a stable fashion throughout the test as they would have been expected to behave in a standard stiff test machine. The only difference between Figures 5 and 6 is that the $T_{material}$ plotted in Figure 5 were calculated from J_I-R curves with crack extension up to 1.5 mm while Figure 6 used $T_{material}$ calculated from J_I-R curves with crack extension up to 5 mm.

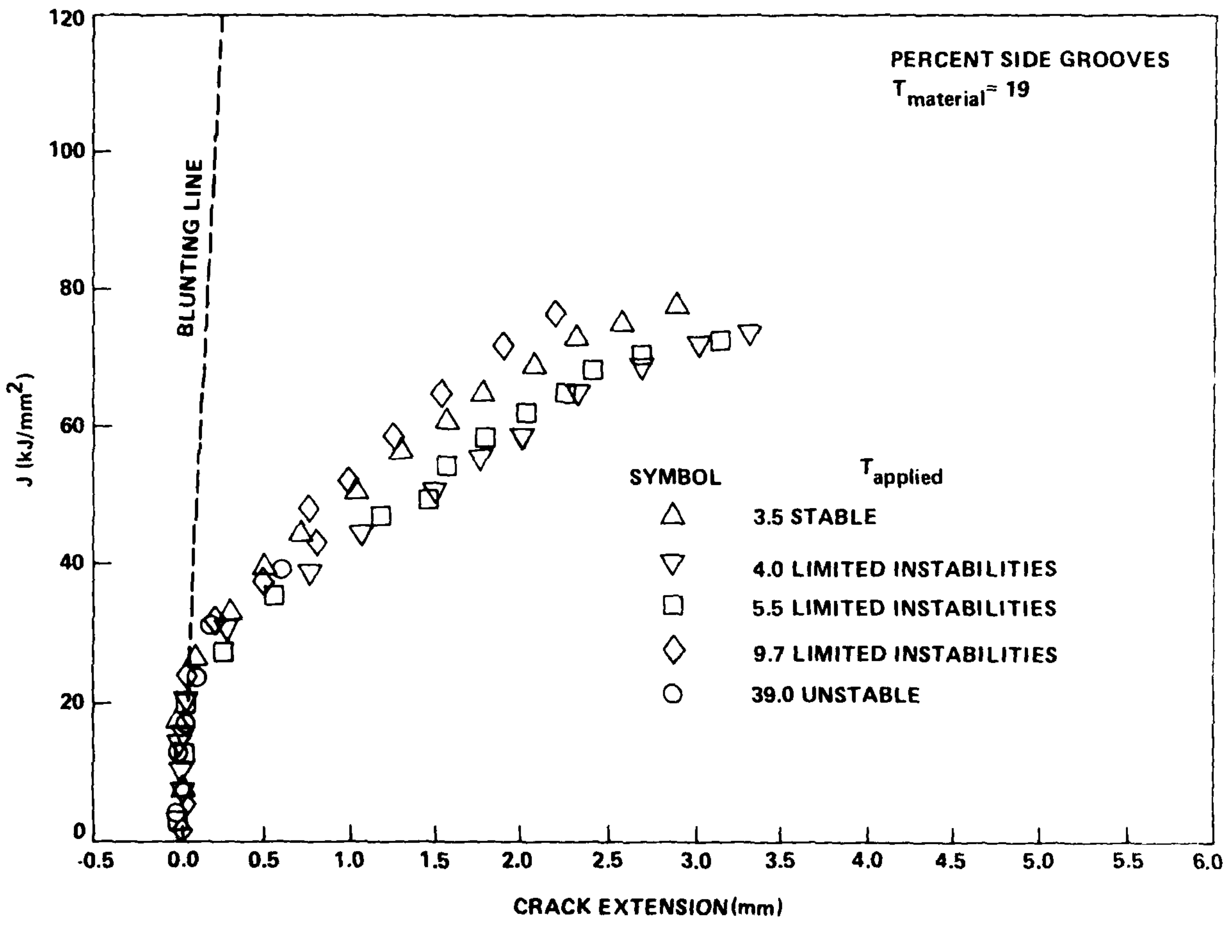

Figure 4 - J_I-R Curves for Non-Side-Grooved 5456-H117 Aluminum Alloy Specimens

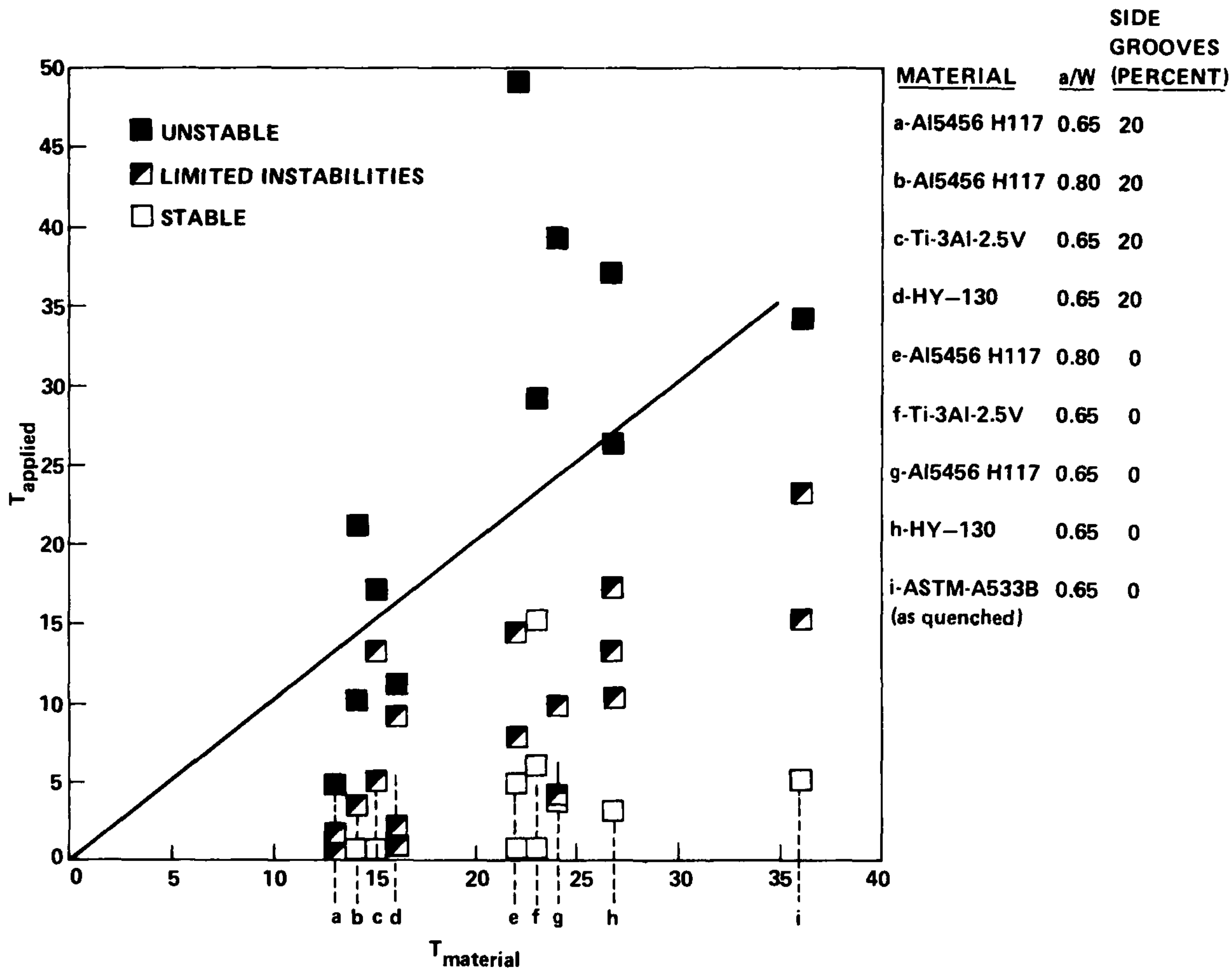

Figure 5 - $T_{applied}$ versus $T_{material}$ with $T_{material}$ Calculated from the J_I-R Curve Slope Taken to a Crack Extension of 1.5 Millimeters

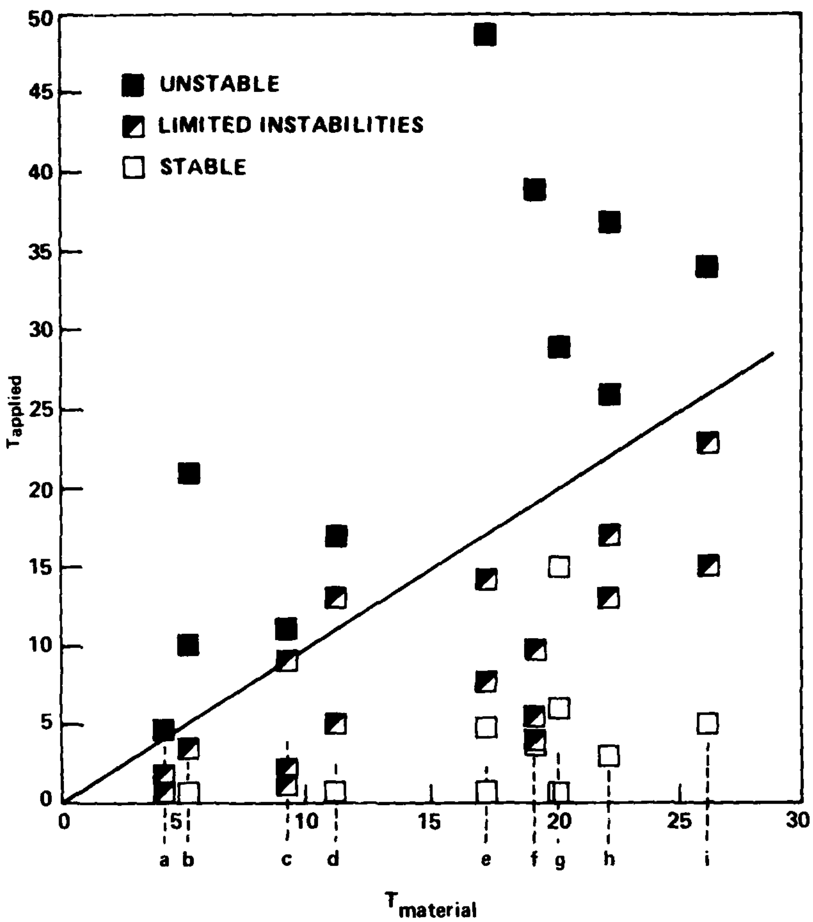

MATERIAL	a/W	SIDE GROOVES (PERCENT)
a-Al5456 H117	0.65	20
b-Al5456 H117	0.80	20
c-HY–130	0.65	20
d-Ti-3Al-2.5V	0.65	20
e-Al5456 H117	0.80	0
f-Al5456 H117	0.65	0
g-Ti-3Al-2.5V	0.65	0
h-HY–130	0.65	0
i-ASTM-A533B (as quenched)	0.65	0

Figure 6 - $T_{applied}$ versus $T_{material}$ with $T_{material}$ Calculated from the J_I-R Curve Slope Taken to Crack Extensions of 5.0 Millimeters

Both Figures 5 and 6 demonstrate the validity of the Paris tearing instability criterion, that when $T_{material} < T_{applied}$ unstable fracture behavior will occur. The two Figures 5 and 6 also show that all the $T_{material}$ calculated from J_I-R curves with crack extension to 5 mm are more accurate measures of the material tearing modulus. This effect was more pronounced on specimens with 20 percent side grooves than on specimens with no side grooves.

The effect of 20 percent side grooves on the materials tested was to produce a different $T_{material}$ from the non-grooved specimens and, correspondingly, to require a different $T_{applied}$ to produce unstable behavior. Figure 6 thus shows that the $T_{material}$ produced with 20 percent side grooved specimens is a real change in the effective material behavior due to the change in constraint. Further research is necessary to prove that the constraint produced by side grooved models is the constraint present in very thick parts.

DISCUSSION OF LIMITED INSTABILITY

In previous work on tearing instability using bend bar specimens, Paris and coworkers[8] did not report observing the wide range of limited instability behavior observed in this work. They did report one case of "marginal behavior" and two other cases termed "stable" that showed instantaneous load drops of about 5 percent just beyond maximum load and possibly some other load drops later in the test - in specimens with $T_{applied} = 0.6 - 0.8\ T_{material}$.

To explain the observed range of limited instability, two possibilities seemed to present themselves. First it was conjectured that $T_{applied}$ would fall rapidly with the increased crack length thus re-establishing stability. The second possibility was that $T_{material}$ varied considerably about the average value obtained by the single specimen J_I-R curve methodology leaving the possibility that occasionally $T_{applied}$ would exceed $T_{material}$ giving a limited instability behavior. To investigate these alternatives, a load-line COD plot was obtained from a non-side-grooved specimen of the HY-130 alloy without any unloadings. Because this alloy was identical to the alloy used by Joyce et al.[17] a "key curve" analysis could be applied to develop a J_I-R curve for this specimen directly from the load displacement curve of the specimen. The resulting J_I-R curve is shown in Figure 7. The key curve analysis result has a $(J,\Delta a)$ pair for each point on the original load displacement curve and thus it allows a determination of the variability in both $T_{material}$ and $T_{applied}$ during a test.

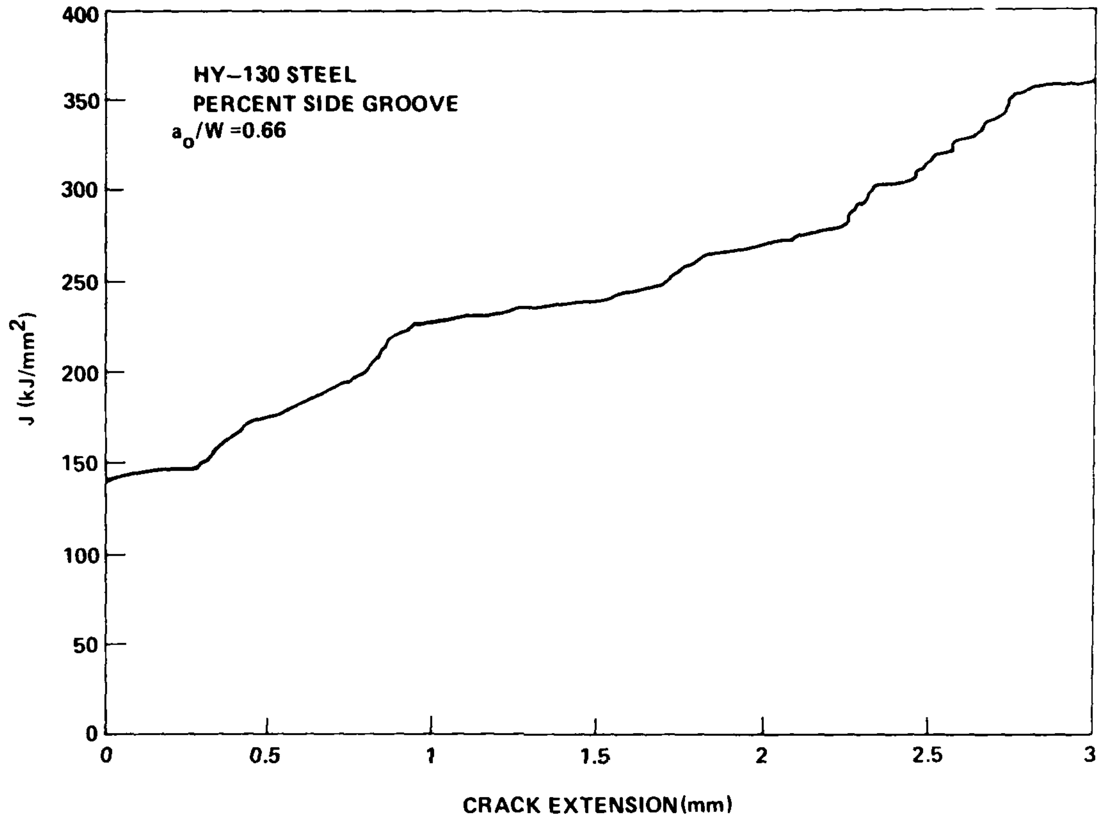

Figure 7 - Key Curve Analysis J_I-R Curve for HY-130 Steel Specimen

Using the J and a/W values defined by the J_I-R curve of Figure 7 allows calculating $T_{applied}$, which would have been present if the test had been run in a compliant test machine with the given stiffness. These results are plotted in Figure 8 and show that $T_{applied}$ does vary during a typical test, but only slowly, decreasing as a/W and J_I increase. No sudden and pronounced reduction in $T_{applied}$ occurs as the result of a slight increase in crack length. If the situation occurred where $T_{applied}$ was slightly above $T_{material}$ at maximum load, a small step of crack extension could occur with stability being reestablished when $T_{applied}$ fell below $T_{material}$. This phenomenon then could not re-occur during this test because $T_{applied}$ would only fall with further increases in a/W or J_I.

To test the second possibility, an iterated quadratic polynomial fit procedure was used to evaluate the local slopes of the J_I-R curve presented in Figure 7, and hence the local $T_{material}$ defined by Equation (1). In the technique used here,

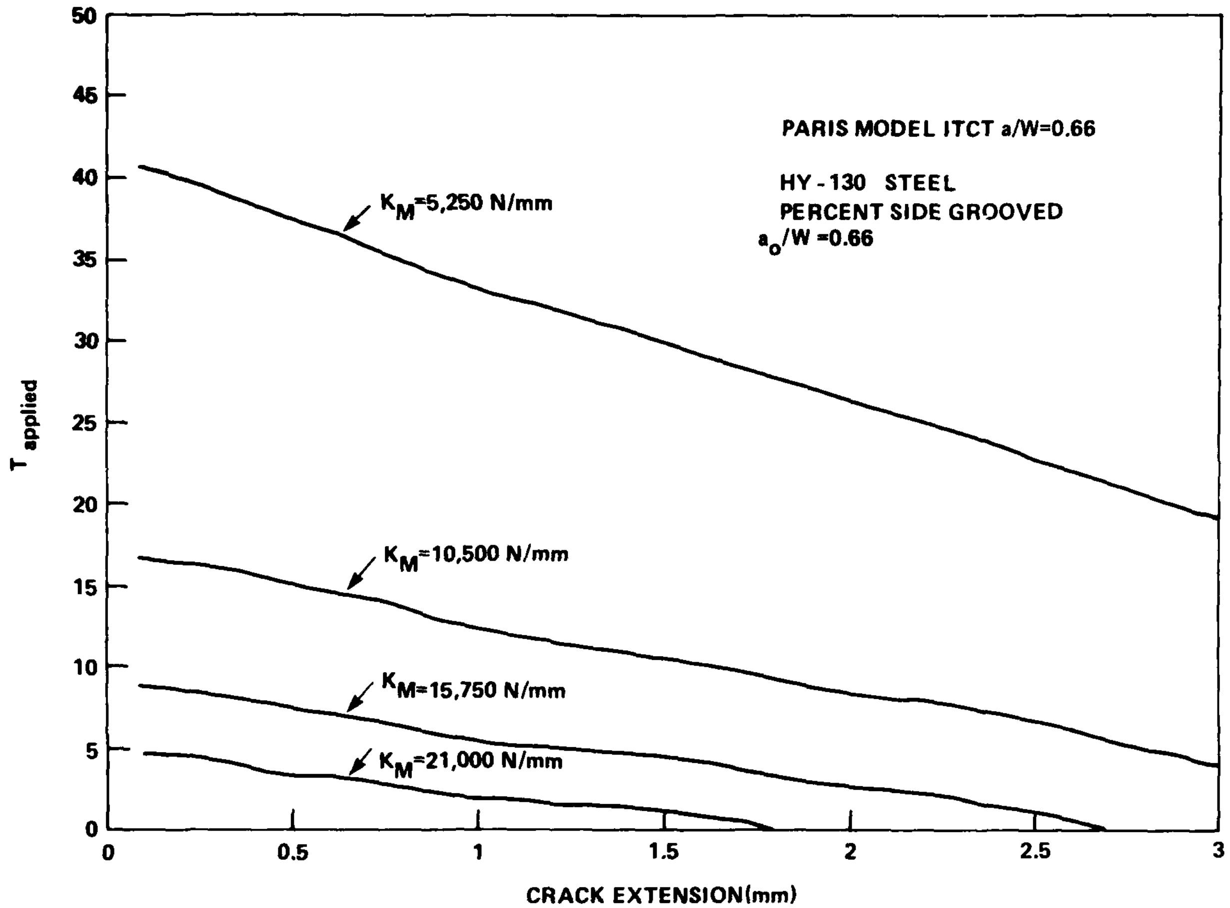

Figure 8 - $T_{applied}$ versus Crack Extension for HY-130 Steel Compact Specimen Tested in a Compliant Test Machine

the polynomial was fit to all J-Δa pairs in a fixed region of Δa instead of to a set number of data points. This procedure, applied to the J_I-R curve of Figure 7, gives the results shown in Figure 9. Here, even when fitting the polynomial over a relatively large region of 0.25 mm of crack extension, a wide band of $T_{material}$ values is found ranging from 5 to 35. Overplotted on this Figure are the $T_{applied}$ curves from Figure 7 which tend to bound the $T_{material}$ scatter band. The implication of this plot is that a mixture of stable and unstable behavior should exist for this material for $T_{applied}$ values ranging from 5 to 35. This effect is not unexpected considering the inhomogeneity of structural materials, producing in turn, irregular crack growth. The wide variation of $T_{material}$ observed here is, however, somewhat surprising.

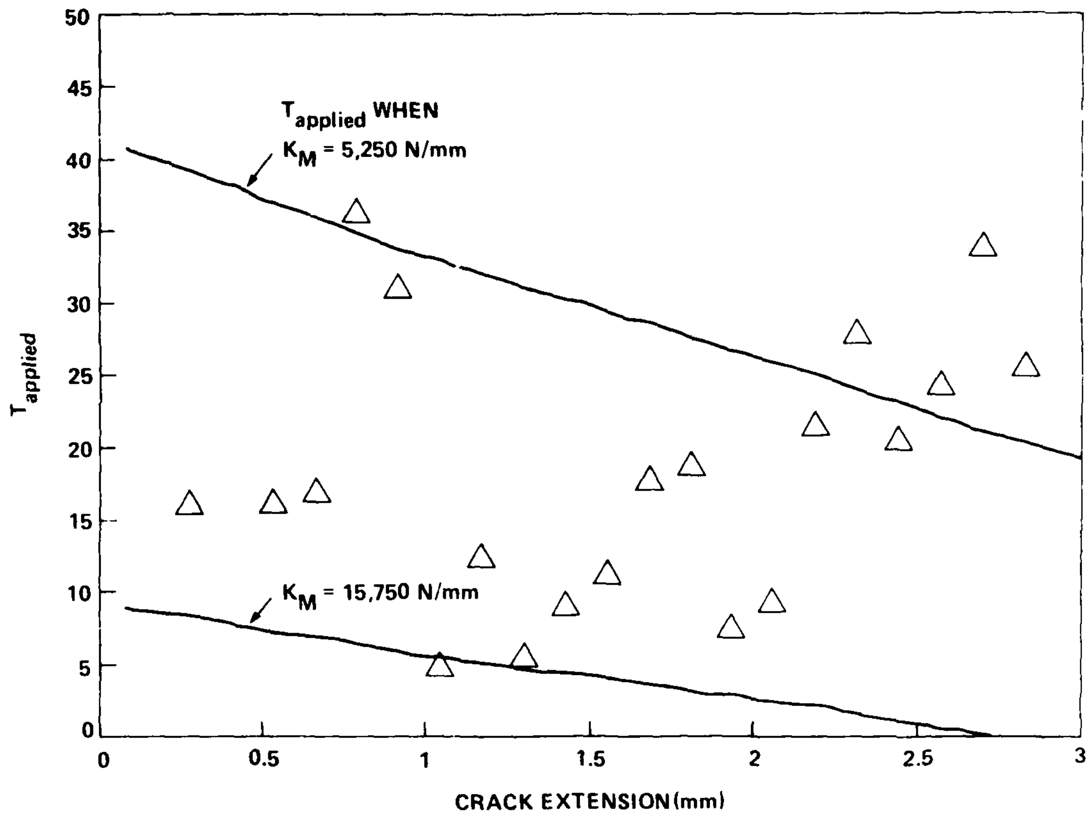

Figure 9 - Local $T_{material}$ Values for HY-130 Steel Alloy Demonstrating Material Variability

CONCLUSIONS

The following conclusions can be drawn from the work described in this report.

- Tearing instability was assured in a compact specimen if the $T_{applied}$ produced by the compliant-test machine exceeded the $T_{material}$ defined by a stable single specimen unloading compliance J_I-R curve for a similar specimen for the range of aluminum, titanium and steel alloys tested here.

- The least squares slope of the J_I-R curve from 0.15 mm beyond the blunting line to a crack extension of 5 mm provided the most accurate measure of $T_{material}$, which, here, was as far as the stable J_I-R curves were measured.

- Macroscopic and scanning electron microscopic analysis showed that the stable and unstable specimen's fracture surfaces were very similar. No evidence of cleavage was observed on fracture surfaces of the unstable specimens.

- In all materials tested, a region of limited instability behavior was observed for a range of $T_{applied}$ below the average $T_{material}$ value, with a gradual reduction in the severity of the unstable behavior as $T_{applied}$ was reduced.

- For $T_{applied}$ less than one tenth the average $T_{material}$, no unstable behavior was observed in these tests.

- The existence of the limited instability region was apparently due to variability of $T_{material}$ about the average value obtained from the single specimen J_I-R curve and not to variations in $T_{applied}$ resulting from the crack extension.

- The J_I-R curves for the materials tested were unaffected by the value of $T_{applied}$ experienced by the compact specimen.

- The added constraint present in the side grooved specimens produced a $T_{material}$ value distinctly different from that of non-side-grooved specimens of the same material. Tearing instability was then controlled by the applicable $T_{material}$ in these specimens.

ACKNOWLEDGMENT

The authors wish to acknowledge Dr. Hendrikus H. J. Vanderveldt of the Naval Sea System Command (NAVSEA 05R15), for supporting this research.

REFERENCES

1. Landes, J.D. and J.A. Begley, "Test Results from J Integral Studies: An Attempt to Establish a J_{Ic} Testing Procedure," in "Fracture Analysis," American Society for Testing and Materials, ASTM-STP-560, pp. 170-186 (1974).

2. Paris, P.C. et al., "The Theory of Instability of the Tearing Mode of Elastic-Plastic Crack Growth," "Elastic-Plastic Fracture," American Society for Testing and Materials, ASTM STP 668, J.D. Landes, J.A. Begley, and G.A. Clarke, eds., pp. 5-36 (1979).

3. Ernst, H., "Techniques of Analysis of Load Displacement Records by J-Integral Methods," PhD Thesis. Sever Institute, Washington Univ., St Louis, Mo. (Aug 1979).

4. Tada, W. et al., "A Stability Analysis of Circumferential Cracks for Reactor Piping System," U.S. Nuclear Regulatory Commission (in preparation).

5. Gudas, J.P. et al., "Investigation of Specimen Geometry Modifications to Determine the Conservative J_I-R Curve Tearing Modulus Using the HY-130 Steel System," in "Fracture Mechanics," American Society for Testing and Materials, ASTM STP 677, C.W. Smith, ed., pp. 474-485 (1979).

6. Vassilaros, M.G. et al., "Effects of Specimen Geometry on the J-R Curve for ASTM A533B Steel," in "Fracture Mechanics," ASTM-STP-700, American Society for Testing and Materials, pp. 251-270 (1980).

7. Joyce, J.A. and J.P. Gudas, "Computer Interactive J_{Ic} Testing of Navy Alloys," in "Elastic-Plastic Fracture," American Society for Testing and Materials, ASTM STP 668, J.D. Landes, J.A. Begley, and G.A. Clarke, eds., pp. 451-468 (1979).

8. Paris, P.C. et al., "Initial Experimental Investigation of Tearing Instability Theory," in "Elastic-Plastic Fracture," American Society for Testing and Materials, ASTM STP 668, J.D. Landes, J.A. Begley, and G.A. Clarke, eds., pp. 251-265 (1979).

9. Clarke, G.A. et al., "A Procedure for the Determination of Ductile Fracture Toughness Values Using J Integral Techniques," Journal of Testing and Evaluation, Vol. 7, No. 1, pp. 49-56 (Jan 1979).

10. Hutchinson, J.W. and P.C. Paris, "Stability Analysis of J-Controlled Crack Growth," in "Elastic-Plastic Fracture," American Society for Testing and Materials, ASTM STP 668, J.D. Landes, J.A. Begley, and G.A. Clarke, eds., pp. 37-64 (1979).

11. Ernst, H. *et al.*, "Estimations of J-Integral and Tearing *Modulus from a* Single Specimen Test Record," presented at the American Society for Testing and Materials 13th National Symposium in Fracture Mechanics, Philadelphia, Pa. (Jun 1980).

12. Hawthorne, J.C. (Ed), "NRL-DPRI Research Program (RP 886-2), Evaluation and Predictions of Neutron Embrittlement in Reactor Pressure Vessel Materials, Annual Progress Report for 1978," Naval Research Laboratory Report 327, p. 40 (30 Aug 1979).

13. Saxena, A. and S. J. Hudak, "Review and Extension of Compliance Information for Corrosion Crack Growth Specimens," "International Journal of Fracture," Vol. 14, pp. 453-468 (1978).

14. Merkle, J.G. and H.T. Corten, "A J-Integral Analysis for the Compact Specimen, Considering Axial Force as Well as Bending Effects," Journal of Pressure Vessel Technology, Transactions of the American Society of Mechanical Engineers, Vol 96, pp. 286-292 (Nov 1974).

15. Paris, P.C., "Fracture Mechanics in the Elastic-Plastic Regime," in Flow Growth and Fracture, American Society for Testing of Materials, pp. 3-27 (1976).

16. Rice, F.R., "Elastic Plastic Fracture Mechanics," in "The Mechanics of Fracture," F. Erdogan, ed., American Society of Mechanical Engineers (1976).

17. Joyce, J.A. et al., "The Direct Evaluation of J. Resistance Curves from Load Displacement Records," in "Fracture Mechanics," ASTM STP 700, American Society of Testing and Materials, pp. 100-111 (1980).

INITIAL DISTRIBUTION

Copies	
1	ONR Code 471
1	NAVMAT 034
4	NRL 1 Code 6000 1 Code 6380 1 Code 6320 1 Code 6396
12	NAVSEA 1 SEA 05D 2 SEA 05R 1 SEA 08 1 SEA 092 2 SEA 323 1 PMS 393 1 PMS 395 1 PMS 396 2 SEA 99612
1	NISC Code 369
12	DTIC

CENTER DISTRIBUTION

Copies	Code	Name
1	17	
1	172	
1	1720.1	
1	28	
1	2802	
1	2803	
1	2809H	
5	281	
2	2811	
21	2814	
1	282	
10	5211.1	Reports Distribution
1	522.1	Unclass Lib (C)
1	522.2	Unclass Lib (A)
2	5231	Office Services

DTNSRDC ISSUES THREE TYPES OF REPORTS

1. DTNSRDC REPORTS, A FORMAL SERIES, CONTAIN INFORMATION OF PERMANENT TECHNICAL VALUE. THEY CARRY A CONSECUTIVE NUMERICAL IDENTIFICATION REGARDLESS OF THEIR CLASSIFICATION OR THE ORIGINATING DEPARTMENT.

2. DEPARTMENTAL REPORTS, A SEMIFORMAL SERIES, CONTAIN INFORMATION OF A PRELIMINARY, TEMPORARY, OR PROPRIETARY NATURE OR OF LIMITED INTEREST OR SIGNIFICANCE. THEY CARRY A DEPARTMENTAL ALPHANUMERICAL IDENTIFICATION.

3. TECHNICAL MEMORANDA, AN INFORMAL SERIES, CONTAIN TECHNICAL DOCUMENTATION OF LIMITED USE AND INTEREST. THEY ARE PRIMARILY WORKING PAPERS INTENDED FOR INTERNAL USE. THEY CARRY AN IDENTIFYING NUMBER WHICH INDICATES THEIR TYPE AND THE NUMERICAL CODE OF THE ORIGINATING DEPARTMENT. ANY DISTRIBUTION OUTSIDE DTNSRDC MUST BE APPROVED BY THE HEAD OF THE ORIGINATING DEPARTMENT ON A CASE-BY-CASE BASIS.

ATE

LMED

-8